Intercomparison of Alternate Soil Moisture Downscaling Algorithms Using Active–Passive Microwave Observations

Xiaoling Wu, Jeffrey P. Walker, Christoph Rüdiger, Rocco Panciera, and Ying Gao

***Abstract*— Three active–passive soil moisture downscaling algorithms are tested to demonstrate the feasibility of each for application to NASA's Soil Moisture Active Passive (SMAP) mission launched in January 2015. These algorithms include the official baseline and optional downscaling algorithms, and a change detection method. These synergistically use 1-km synthetic aperture radar backscatter to downscale 36-km brightness temperature to 9 km, which is then converted into soil moisture at 9 km, or downscale soil moisture directly to 9-km resolution. While these algorithms have been tested previously, this was mostly using synthetic data sets. Moreover, there has never before been a direct comparison of the alternate methods using the same data sets. Thus, it is imperative that they be tested against each other for a comprehensive range of land surface conditions prior to global application. Consequently, this letter evaluates these three algorithms using data collected from the soil moisture active passive experiments (SMAPExs) in Australia, designed to closely simulate the SMAP data stream for a single SMAP radiometer pixel over a three-week interval. Results suggested that the average root-mean-square error (RMSE) in downscaled soil moisture at 9-km resolution was 0.019, 0.021, and 0.026 cm^3/cm^3 for the baseline, optional, and change detection method, respectively. While there was a little difference in the RMSE, the optional method showed the best correlation between the downscaled soil moisture and the reference soil moisture map. Therefore, the optional algorithm is recommended for global implantation by SMAP.**

***Index Terms*— Active–passive, downscaling algorithms, soil moisture, soil Moisture active Passive (SMAP), soil moisture active passive experiments (SMAPExs).**

I. Introduction

THE global measurement of soil moisture is vital to understanding the components and interactions of the global water, energy, and carbon cycles, and therefore benefit applications in agriculture, hydrology, and meteorology [1]. Methods are being developed to make use of emerging remotely sensed soil moisture information to constrain numerical model prediction of soil moisture [2], and hence improve the forecasting of weather, floods, and agriculture-related applications, leading to significant societal benefits.

The passive microwave remote sensing has been generally accepted as the most accurate of the remote sensing methods for soil moisture mapping, due to its stronger and more direct connection between the observed brightness temperature (Tb) and the surface soil moisture (∼5 cm), than with radar backscatter obtained using active microwave sensing or thermal data [3]. The best results were found at low frequency (∼1.4 GHz) due to reduced interference by the atmosphere, surface roughness, and vegetation. Consequently, the Soil Moisture and Ocean Salinity mission [4] was launched by the ESA in November 2009, as the first-ever satellite dedicated to soil moisture measurement using the *L*-band passive microwave measurements. However, it suffers from being relatively low spatial resolution (around 36 km), which, therefore, is a significant limitation for regional applications, such as precipitation forecasting and flood prediction. While fine-scale soil moisture information can be retrieved by active microwave remote sensing, the observations are less sensitive to changes in soil moisture due to the confounding effects of vegetation conditions and surface roughness. Consequently, NASA's Soil Moisture Active Passive (SMAP) mission [5], launched in January 2015, aims to overcome this scale issue by using fine-scale (3 km) active microwave observations to downscale the coarse-scale (36 km) passive microwave observations to medium (9 km) resolution. The synergy between active and passive observations may overcome the limitations of each observation individually, ultimately providing soil moisture data at a resolution more suitable for hydrometeorological applications.

In preparation for operational delivery of downscaled soil moisture from combined SMAP radiometer and radar observations, suitable algorithms need to be developed and validated. Those algorithms include the proposed baseline downscaling method [6], [7] and the optional method for SMAP [7], [8], and a change detection method [9], [10].

Given that the current downscaling algorithms are relatively immature and not widely tested using experimental data, the main objective of this letter is to evaluate these three linear downscaling algorithms using active and passive observations from the Soil Moisture Active Passive Experiment (SMAPEx) field campaigns undertaken in Australia [11]. The SMAPEx provides the opportunity to evaluate the SMAP active–passive

Manuscript received December 14, 2015; revised April 1, 2016; accepted October 12, 2016. Date of publication December 15, 2016; date of current version January 19, 2017. This work was supported in part by the Australian Research Council Discovery under Grant DP0984586 and in part by Infrastructure under Grant LE0453434 and Grant LE0882509.

X. Wu, J. P. Walker, C. Rüdiger, and Y. Gao are with the Department of Civil Engineering, Monash University, Clayton, VIC 3800, Australia (e-mail: xiaoling.wu@monash.edu; jeff.walker@monash.edu; chris.rudiger@monash.edu; ying.gao@monash.edu).

R. Panciera is with the Cooperative Research Centre for Spatial Information, The University of Melbourne, Melbourne, VIC 3053, Australia (e-mail: panceraroco@gmail.com).

Color versions of one or more of the figures in this letter are available online at http://ieeexplore.ieee.org.

Digital Object Identifier 10.1109/LGRS.2016.2633521

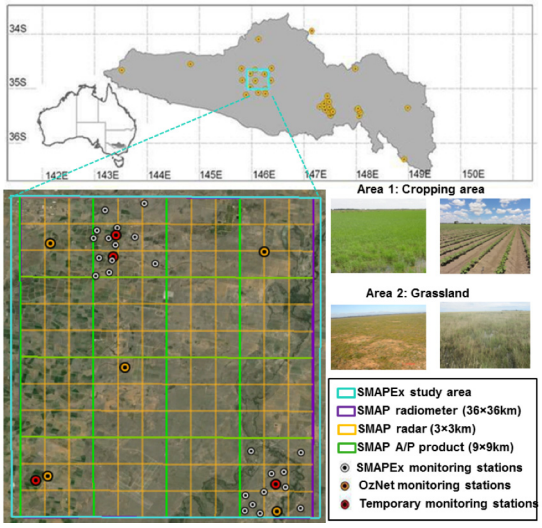

Fig. 1. Overview of the SMAPEx site showing the SMAP pixel sized study site, and the SMAP grid on which the 36-km resolution radiometer data, 3-km resolution radar data, and 9-km resolution active–passive downscaled product will be provided.

baseline algorithms using data that present with different surface conditions and land cover. Importantly, this is the first study to make a direct intercomparison of the three algorithms using the experimental data.

II. Data Set

The SMAPEx study area, with a size of approximately 38 km × 36 km, is situated within the Murrumbidgee River catchment, as shown in Fig. 1. It was chosen for testing the performance of SMAP downscaling algorithms due to its flat topography, high density of soil moisture monitoring stations, and the spatial variability in soil, vegetation, and land use, allowing an investigation of the downscaling algorithms under unique geophysical and meteorological conditions that are so far not tested for this purpose. The western part of the SMAPEx site is dominated by cropping areas, while the eastern half consists mostly of grassland areas. The SMAPEx airborne instrument suite consists of the polarimetric L-band multibeam radiometer (PLMR) and the polarimetric L-band imaging synthetic aperture radar (PLIS), so as to provide an SMAP-like data stream for developing and testing of the algorithms applicable to the SMAP mission viewing configuration. A complete description of the experiment design can be found in [11]. The radiometer and radar data were from the third SMAPEx campaign (SMAPEx-3, September 5–23, 2011), which was conducted during the spring vegetation growing season. This campaign was used, since it comprised nine regional flights over a three-week time period with the two to three days revisit time of SMAP.

In order to closely replicate the prototype SMAP data stream, data collected during the campaigns were processed in terms of resolution aggregation and incidence-angle normalization [12]. The original resolutions of the data were 1 km for the PLMR Tb and 10–30 m for the PLIS backscatter. PLMR data were linearly aggregated to 36 and 3 km, while the PLIS data were aggregated to 1 and 9 km to evaluate the performance of the SMAP downscaling algorithm if applied at different resolutions. In terms of the number of pixels, one at 36-km scale, 16 at 9-km scale, and 1296 at 1-km scale were used in this letter. The reference used to evaluate the downscaling results came from the 1-km PLMR retrieved soil moisture, which has been validated against the ground sampled soil moisture, with an accuracy of 0.06 m^3/m^3 in cropland and 0.05 m^3/m^3 at grassland according to [13]. The reference data were also aggregated to resolutions of 3 and 9 km, in order to evaluate the efficiency of each downscaling algorithm at different resolution levels.

III. Methodology

A. Baseline Downscaling Algorithm

The baseline downscaling algorithm to be implemented by SMAP is based on the assumption of a near-linear relationship between Tb and σ [6], [7], [14]. In the following, the naming convention of "C" (coarse) and "F" (fine) represents 36- and 3-km resolutions. Implementation of this method requires a background Tb at coarse resolution, with the variation of Tb imposed by the distribution of fine scale σ modulated by the sensitivity parameter β_1 of the linear regression between Tb and σ at coarse resolution, according to

$$\mathrm{Tb}_p(F_j) = \mathrm{Tb}_p(C) + \beta_1(C) \times \{[\sigma_{pp}(F_j) - \sigma_{pp}(C)] + \Gamma \times [\sigma_{pq}(C) - \sigma_{pq}(F_j)]\} \quad (1)$$

where p indicates the polarization, including h- and v-pol; and pp means copolarization of radar observations σ, including hh- or vv-pol; and pq represents hv-pol. $\mathrm{Tb}_p(F_j)$ is the brightness temperature value of a particular pixel "j" of resolution F, and $\sigma_{pp}(F_j)$ is the corresponding radar backscatter value of pixel "j." Γ is a sensitivity parameter for each particular grid cell C and season defined as $\Gamma = [\delta\sigma_{pp}(F_j)/\delta\sigma_{pq}(F_j)]_C$. The output of this baseline downscaling algorithm is the downscaled Tb, with details described in the previous study done by Wu *et al.* [15]. Therefore, the main work concerning this downscaling algorithm in this letter is to interpret the obtained downscaled Tb to the downscaled soil moisture product, using the tau–omega ($\tau - \omega$) passive microwave retrieval algorithm with soil and vegetation parameters [16], [17].

B. Optional Downscaling Algorithm

The optional downscaling algorithm [8] for SMAP is similar to the baseline algorithm, but uses the soil moisture instead of Tb in (1). Implementation of this method requires a background soil moisture θ at C resolution, with the variation of θ imposed by the distribution of fine scale σ within C modulated by $\beta_2(C)$ of the linear regression between θ and σ at C resolution according to

$$\theta(F_j) = \theta(C) + \beta_2(C) \times \{[\sigma_{pp}(F_j) - \sigma_{pp}(C)] - \Gamma \times [\sigma_{pq}(C) - \sigma_{pq}(F_j)]\} \quad (2)$$

where $\theta(F_j)$ is the soil moisture of a particular pixel "j" of resolution F, $\theta(C)$ aggregated from a 1-km resolution PLMR retrieved soil moisture product (through the passive microwave retrieval algorithm). $\beta_2(C)$, which is also assumed

to be time-invariant and homogenous over the entire 9-km pixel, is obtained through the time-series of $\theta(C)$ and $\sigma_{pp}(C)$. Other terms in (2) are the same as (1). The main differences between the optional and baseline downscaling algorithms are: 1) estimation of the sensitivity parameter β from θ and σ (optional) rather than from Tb and σ (baseline) and 2) soil moisture retrieved in a direct (optional) rather than an indirect (baseline) way; the latter needs the downscaled Tb to go into the $\tau - \omega$ retrieval model.

C. Change Detection Method

The change detection method assumes a linear relationship between the temporal change of radar backscatter and temporal change of soil moisture at the same spatial scale [9]. It has the same assumption as the optional algorithm, but is different in retrieving medium resolution soil moisture

$$\theta(F_j, t) = \theta(C, t - t_R) + \beta_3(C) \times \{\sigma_{pp}(F_j, t) - \sigma_{pp}(F_j, t - t_R)\} \quad (3)$$

where $\theta\ (F_j, t)$ is the soil moisture of a particular pixel "j" of resolution F and at time t and $\theta\ (C,\ t\text{-}t_R)$ is aggregated from the 1-km resolution PLMR retrieved soil moisture product at time $t\text{-}t_R$, where t_R is the revisit time of the observations; two to three days for the SMAP case. $\theta(C,\ t\text{-}t_R)$ is then updated with the soil moisture change evident in the fine resolution radar backscatter σ at the two different times. $\beta_3(C)$, which is also assumed to be time-invariant and homogenous over the entire site, is obtained through the time-series of $\theta(C)$ and $\sigma_{pp}(C)$. While the optional algorithm is based on a background soil moisture value with the variation across the entire area characterized by radar observations, the change detection method assumes that a soil moisture estimate at a given time can be obtained according to the previous soil moisture estimate plus the change in soil moisture, given by the radar observations and the regression slope β_3.

IV. Results and Discussion

For the baseline algorithm, β was estimated from Tb and σ at 36-km resolution. As stated in [15], σ at vv-pol showed the best correlation with Tb and was used for estimating β_1. Therefore, β_1 was calculated at h- and v-pol, being -3.4 and -2.2 K/dB, respectively. Different to the baseline algorithm, the sensitivity of soil moisture to backscatter in the optional algorithm was analyzed using the slope of the linear regression as a measure of quality and, therefore, the parameter β_2 was obtained, being 0.018 cm^3/cm^3/dB. Since β_3 of the change detection method is also the sensitivity of soil moisture to backscatter, the same value as β_2 was used. According to the previous work done by Wu *et al.* [14], [15], the magnitude of β was actually affected by the land cover types, vegetation biomass, and the existence of water bodies. Therefore, the assumption of a constant β in this letter may influence the resulting accuracy of the downscaled product when compared with the reference.

Since the observed σ from radar is not only related to the soil moisture, but also to the vegetation conditions, the use of Γ in the baseline and optional downscaling algorithm aims to reduce the influence of vegetation on σ and to make it more strongly correlated to the soil moisture. The study area was divided into 16 subareas of 9 km by 9 km in size, and the value of Γ calculated using the snapshots of all σ_{vv}–σ_{hv} pairs at 1-km resolution contained within each of those subareas, allowing an analysis of the relationship between the estimation of Γ and vegetation conditions. Γ ranges from 0.2–0.45 according to different vegetation conditions.

The downscaled θ from three algorithms was retrieved at resolutions of 1, 3, and 9 km, from linearly aggregating the 1-km resolution downscaled θ to 3- and 9-km resolution. The accuracy of these three downscaling algorithms was evaluated against the reference soil moisture θ, being the PLMR retrieved soil moisture at 1-km resolution [13]. The downscaled results of the baseline and optional algorithms are similar in terms of the root-mean-square error (RMSE). For the baseline algorithm, the average RMSE across the nine days was 0.038, 0.028, and 0.019 cm^3/cm^3 at 1-, 3-, and 9-km resolution, respectively. The average RMSE for the optional algorithm differed by only 0.002–0.003 cm^3/cm^3 depending on the resolution. In comparison, the change detection method had the largest RMSE, being 0.006 cm^3/cm^3 larger than the baseline algorithm. One possible reason contributing this relatively poor performance of the change detection method is the unaccounted influence from the vegetation. Unlike the baseline or optional methods, the change detection method does not use σ_{hv} and the parameter Γ to compensate for the influence of vegetation on the soil moisture retrieval.

The RMSE of each algorithm generally decreased from the beginning to the end of the nine days. Results of the first days, i.e., D1 to D3 displayed relatively poor performance, when compared with the later days. One possible reason is attributed to the heavy rainfall events that led to wet soil and vegetation conditions in the northeastern part of the study area at the beginning of SMAPEx-3, subsequently impacting the radiometer and radar observations. Since Tb was more sensitive to the immediate soil moisture changes due to the rain in this region, the value of Tb drop according to soil moisture increase was more significant than the radar backscatter changes, as the latter are more influenced by the vegetation cover and consequently less sensitive to the soil moisture changes. Consequently, the sensitivity of backscatter to Tb/θ decreases, resulting in an obvious difference in the sensitivity parameter β for the area subjected to rainfall when compared with the other drier areas, which would have dominated the derivation of β itself. The influence on surface heterogeneity due to the rain event decreased during the dry-down period, especially after D3, as shown through the decrease in RMSE from D3 onward. In terms of resolution, there is an obvious reduction of RMSE when applied to a larger scale, e.g., from 1 km to 3 and 9 km, respectively, which can be attributed to the reduction of random (white) noise following the aggregation of the backscatter data.

Intercomparison of three downscaling algorithms on D8 is shown in Fig. 2 as an example of the results. The pattern of the optional algorithm largely matched that of the reference, the change detection method could hardly represent the actual

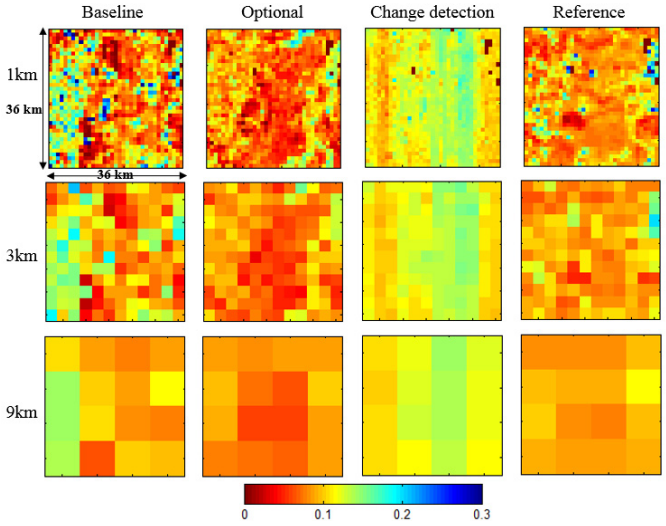

Fig. 2. Example comparison of downscaled soil moisture maps (cm^3/cm^3) from each downscaling algorithm (baseline, optional, and change detection) and the reference at different resolutions (1, 3, and 9 km). Data were collected on D8 (September 21, 2011) of SMAPEx-3. Pixels at 1-km resolution in the northeast of the study area are the water bodies, which have been removed prior to conducting the downscaling.

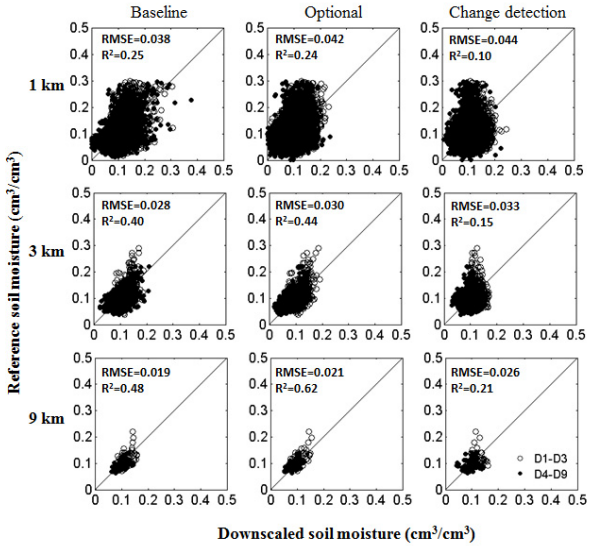

Fig. 3. Comparison between reference and downscaled soil moisture maps from the baseline, optional, and change detection method at 1-, 3-, and 9-km resolution. Performance of each method was evaluated in terms of RMSE (in unit of cm^3/cm^3) and correlation (R^2) between downscaled and reference soil moisture. Data are from all nine days of SMAPEx-3, with data from days 1–3 denoted by circles, and data from days 4–9 denoted by solid circles.

pattern, and the baseline algorithm showed a similar pattern to the reference but with poorer performance than for the optional algorithm. Although each of these three downscaling algorithms had similar RMSE, their ability to correctly detect the soil moisture pattern as shown in the reference map was considerably different; this is another key factor in examining the performance of the downscaling algorithms.

In order to quantify the degree of pattern match, a further evaluation of the skill of each algorithm was undertaken, through the examination of the correlation (R^2) between downscaled and reference θ (see Fig. 3) using all nine days of data. It is noted that the correlation at 1 km was quite poor for all algorithms, primarily due to the high noise level of the

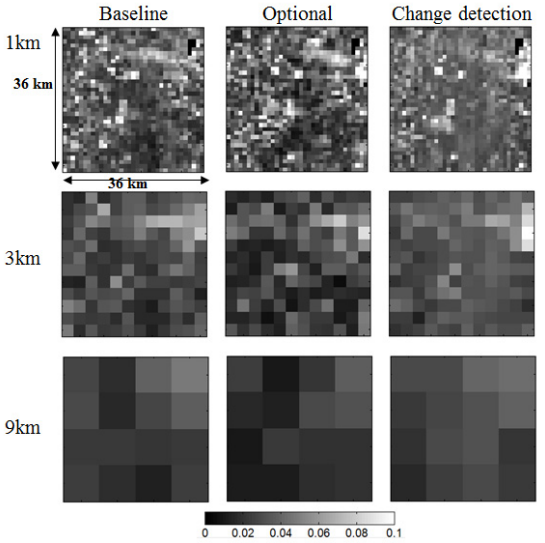

Fig. 4. Spatial distribution of RMSE for baseline algorithm, optional algorithm, and change detection method across the entire SMAPEx site at 1-, 3-, and 9-km resolution. RMSE for each pixel was calculated from the downscaled soil moisture and the reference at this pixel across the nine days.

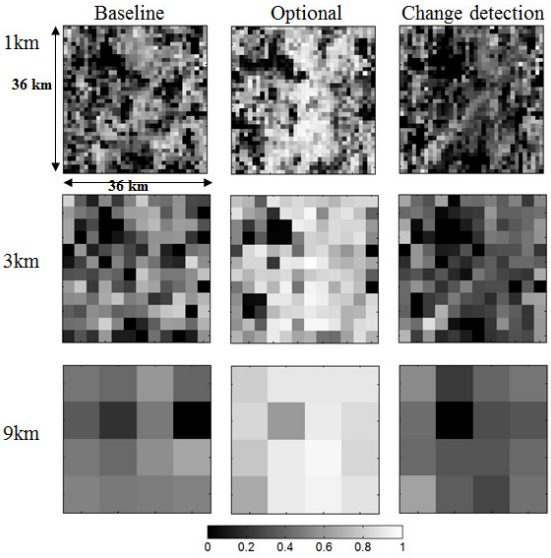

Fig. 5. Spatial distribution of correlation coefficient (R^2) for baseline, optional, and change detection method across the entire SMAPEx site at 1-, 3-, and 9-km resolution. R^2 for each pixel was calculated from the downscaled soil moisture and the reference at this pixel across the nine days.

radar observations at 1 km; the correlation was improved by approximately 0.23, 0.48, and 0.11, respectively, for baseline, optional, and change detection method, when observations were averaged to 9 km. One limitation for this letter was only nine days' of data were available and that the size of the study area was relatively small, limiting the number of pixels that could be analyzed. However, the results from different methods are still comparable. By comparing the behavior of each algorithm at 9-km resolution, the optional algorithm showed the best correlation with the reference at around 0.62, being approximately 0.14 higher than the baseline; the change detection algorithm was observed to have the poorest correlation between its retrieved soil moisture and the reference, around 0.21, when compared with the other.

In order to differentiate the impact from land cover types on the downscaling performance, the spatial distribution of the RMSE and the correlation coefficient R^2 was also obtained at different spatial resolutions across the entire study area, as shown in Figs. 4 and 5. Both RMSE and R^2 were calculated from the series of downscaled soil moisture and the reference at each pixel across nine days, and at three resolution levels. As shown in Fig. 4, the optional and baseline downscaling algorithms showed minor difference in terms of the spatial plot of RMSE, but overall these two were better than the change detection method. It is noted that at 1 km, a number of pixels have an error as large as 0.10 cm^3/cm^3, being attributed to the weak linear relationship between backscatter and Tb at 1 km and also the noisy radar data at 1 km which got cancelled out when upscaled to 3 and 9 km. It is observed that the left side of the study area dominated by crops had greater error than the middle part that was occupied by grasslands, indicating the higher heterogeneity in the croplands attributed to a worse performance of downscaling. Moreover, the northeast area also had poor performance, probably due to the increased surface heterogeneity as a consequence of raining events during the first couple days. The optional downscaling algorithm had the best correlation, as shown in Fig. 5, in line with the results in Fig. 3. Although the water bodies have been removed prior to downscaling, there are a fair number of pixels in Fig. 5 where the correlation coefficient is near zero. This was probably due to irrigation activities in the cropping areas. The croplands, which had more variations in the vegetation conditions, surface roughness, and row structure, will also have impacted the radar observations and, therefore, hampered the accuracy of downscaling. The forests, mainly distributed in the eastern part of the study site, may also have impacted on the correlation. The more homogenous grasslands had overall better performance in downscaling with lower RMSE and higher correlation to the soil moisture truth.

V. Conclusion

The objective of this letter was to test the robustness of three downscaling algorithms using active and passive observations from the SMAPEx field campaign in Australia. Errors associated with each algorithm were assesed for different spatial resolutions. The average RMSE of downscaled soil moisture at 9-km resolution was 0.019, 0.021, and 0.026 cm^3/cm^3 for baseline, optional, and change detection method, respectively. All three algorithms were found to perform poorly in the early days of the experiment due to large rainfall events in the study area that created a large spatial heterogeneity in terms of soil moisture content. In contrast, the last six days of the experiment, characterized by a drying down period and no rainfall, showed an improvement in the algorithm performance, with an RMSE consistently better than 0.02 cm^3/cm^3 at 9-km resolution. However, apart from the RMSE, the ability to detect the soil moisture spatial pattern is also an essential factor for examining the performance of each algorithm. After looking at the patterns in retrieved soil moisture, the change detection method showed the poorest results while the optional algorithm was best in representing the correct soil moisture pattern under dry surface conditions. Thus, by assessing RMSE and the correlation between downscaled soil moisture and reference, the optional downscaling algorithm was found to have the best performance and is, therefore, recommended for use in SMAP.

Acknowledgment

The authors would like to thank the collaboration of a large number of scientists from throughout Australia and around the world, and in particular key personnel from the SMAP Team, which provided significant contribution to the campaign's design and execution.

References

[1] W. Wagner *et al.*, "Evaluation of the agreement between the first global remotely sensed soil moisture data with model and precipitation data," *J. Geophys. Res. Atmos.*, vol. 108, no. D19, p. 4611, 2003.

[2] X. K. Shi *et al.*, "Application of satellite microwave remote sensed brightness temperature in the regional soil moisture simulation," *Hydrol. Earth Syst. Sci. Discussions*, vol. 6, no. 1, pp. 1233–1260, 2009.

[3] Y. H. Kerr, "Soil moisture from space: Where are we?" *Hydrogeol. J.*, vol. 15, no. 1, pp. 117–120, 2007.

[4] Y. H. Kerr *et al.*, "The SMOS mission: New tool for monitoring key elements of the global water cycle," *Proc. IEEE*, vol. 98, no. 5, pp. 666–687, May 2010.

[5] D. Entekhabi *et al.*, "The soil moisture active passive (SMAP) mission," *Proc. IEEE*, vol. 98, no. 5, pp. 704–716, May 2010.

[6] N. N. Das, D. Entekhabi, E. G. Njoku, J. J. C. Shi, J. T. Johnson, and A. Colliander, "Tests of the SMAP combined radar and radiometer algorithm using airborne field campaign observations and simulated data," *IEEE Trans. Geosci. Remote Sens.*, vol. 52, no. 4, pp. 2018–2028, Apr. 2014.

[7] D. Entekhabi *et al.*, *Algorithm Theoretical Basis Document: L2 & L3 Radar/Radiometer Soil Moisture (Active/Passive) Data Products, Initial Release, Version 1*, accessed on 2012. [Online]. Available: http://smap.jpl.nasa.gov/files/smap2/L2&3_SM_AP_InitRel_v11.pdf

[8] N. N. Das, D. Entekhabi, and E. G. Njoku, "An algorithm for merging SMAP radiometer and radar data for high-resolution soil-moisture retrieval," *IEEE Trans. Geosci. Remote Sens.*, vol. 49, no. 5, pp. 1504–1512, May 2011.

[9] M. Piles, D. Entekhabi, and A. Camps, "A change detection algorithm for retrieving high-resolution soil moisture from SMAP radar and radiometer observations," *IEEE Trans. Geosci. Remote Sens.*, vol. 47, no. 12, pp. 4125–4131, Dec. 2009.

[10] U. Narayan, V. Lakshmi, and T. J. Jackson, "High-resolution change estimation of soil moisture using L-band radiometer and radar observations made during the SMEX02 experiments," *IEEE Trans. Geosci. Remote Sens.*, vol. 44, no. 6, pp. 1545–1554, Jun. 2006.

[11] R. Panciera *et al.*, "The soil moisture active passive experiments (SMAPEx): Toward soil moisture retrieval from the SMAP mission," *IEEE Trans. Geosci. Remote Sens.*, vol. 52, no. 1, pp. 490–507, Jan. 2014.

[12] X. Wu, J. P. Walker, C. Rüdiger, R. Panciera, and D. A. Gray, "Simulation of the SMAP data stream from SMAPEx field campaigns in Australia," *IEEE Trans. Geosci. Remote Sens.*, vol. 53, no. 4, pp. 1921–1934, Apr. 2015.

[13] Y. Gao *et al.*, "Evaluation of the tau-omega model for passive microwave soil moisture retrieval using SMAPEx data sets," *IEEE Trans. Geosci. Remote Sens.*, submitted for publication.

[14] X. Wu, J. P. Walker, C. Rüdiger, and R. Panciera, "Effect of land-cover type on the SMAP active/passive soil moisture downscaling algorithm performance," *IEEE Geosci. Remote Sens. Lett.*, vol. 12, no. 4, pp. 846–850, Apr. 2015.

[15] X. Wu, J. P. Walker, N. N. Das, R. Panciera, and C. Rüdiger, "Evaluation of the SMAP brightness temperature downscaling algorithm using active–passive microwave observations," *Remote Sens. Environ.*, vol. 155, pp. 210–221, Dec. 2014.

[16] T. J. Jackson, T. J. Schmugge, and J. R. Wang, "Passive microwave sensing of soil moisture under vegetation canopies," *Water Resour. Res.*, vol. 18, no. 4, pp. 1137–1142, 1982.

[17] T. J. Jackson and T. J. Schmugge, "Vegetation effects on the microwave emission of soils," *Remote Sens. Environ.*, vol. 36, no. 3, pp. 203–212, Jun. 1991.